

# Stochastic Comparisons of Probability Distribution Functions with Experimental Data in a Liquid-Liquid Extraction Column for the Determination of Drop-Sized Distributions

Sh. Houshyar<sup>1</sup>, M. Torab-Mostaedi<sup>2\*</sup>, S. M. A. Moosavian<sup>1</sup>, S. H. Mousavi<sup>1</sup>, M. Asadollahzadeh<sup>2</sup>

<sup>1</sup> School of Chemical Engineering, Faculty of Engineering, University of Tehran, Tehran, Iran

<sup>2</sup> Materials and Nuclear Fuel Research School, Nuclear Science and Technology Research Institute, Tehran, Iran

---

## ARTICLE INFO

### Article history:

Received: 2016-09-01

Accepted: 2016-10-10

---

### Keywords:

Liquid-liquid Extraction Column

Sauter-Mean Drop

Diameter

Drop-Sized Distribution

Liquid-Liquid Extraction

---

## ABSTRACT

The droplet-sized distribution in the column is usually represented as the average volume-to-surface area, known as the Sauter-mean drop diameter. It is a key variable in the extraction column design. A study of the drop-sized distribution and Sauter-mean drop diameter for a liquid-liquid extraction column has been presented for a range of operating conditions and three different liquid-liquid systems. The effects of rotor speed and dispersed and continuous phase velocities on drop-sized distribution are investigated. Drop-sized distribution is appropriately described using the normal and log-normal probability density functions. The mathematical approach is used to determine the constant parameters in these functions and to provide the fit of the experimental data with them. In addition, empirical expressions are derived to predict the parameters of the distribution curve as a function of operating variables and physical properties of the systems. Good agreement between the outcomes of both the prediction and experiments was achieved for all the investigated operating conditions. An empirical correlation is also proposed to predict the Sauter-mean drop diameter with mean deviation of 9.8 %.

---

## 1. Introduction

Various types of liquid-liquid extraction columns have been used on a commercial scale for a range of applications in the hydrometallurgical, pharmaceutical, chemical, and nuclear industries [1,2]. The Scheibel extraction column, originally intended as an alternative to provide a large number of stages in a single unit, was first described by Scheibel in 1984 [3]. This

column is a kind of mechanically agitated column, consisting of an alternate series of mixing zones and packing sections; the packing section isolates the agitator flow patterns between adjacent stages, thus reducing back-mixing and inducing the coalescence of the droplets and separation of the phases [4-6].

Knowledge of the drop-sized distribution is of paramount importance in the design and

---

\*Corresponding author: mmostaedi@aeoi.org.ir

operation of solvent extraction columns. It affects the dispersed phase holdup, residence time of the droplets, and maximum capacity of the column [7,8]. Furthermore, drop-sized together with dispersed phase holdup provides a measure of the interfacial area. Therefore, it is important to be able to predict the drop diameter for any given system as a function of the operating conditions, physical properties of the systems, and column geometry.

The mean drop-sized correlations of various rotating columns are illustrated in Table 1. However, the available correlations for the

prediction of mean drop-sized distributions are either approximate or scarcely applicable.

At present, little information is existant in the literature regarding the drop-sized distribution in Scheibel extraction column.

In the present study, the drop-sized distributions are measured over a range of operating conditions using a 113 mm diameter Scheibel column for three different liquid systems. The experimental results are then compared to the previous correlations. An empirical expression is developed to predict the Sauter-mean diameter based on the experimental and literature data.

**Table 1**

Unified correlations for the prediction of the drop-sized distribution in mechanically agitated columns.

Equation	Column	Reference
For $Re \leq 50000$	(2) Rotating disc column	[9]
$\frac{d_{32}}{D_c} = 0.18 \left( \frac{ND_c^2 \rho_c}{\mu_c} \right)^{-1.12} \left( \frac{\mu_c}{\sqrt{\sigma \rho_c D_c}} \right)^{-1.38} \left( \frac{\Delta \rho}{\rho_c} \right)^{-0.24} \left( \frac{D_c^2 \rho_c g}{\sigma} \right)^{-0.05} \left( \frac{h}{d_R} \right)^{0.42}$		
$\frac{d_{32}}{H} = \frac{C_\psi e^n}{\frac{1}{C_\Omega \left( \frac{\sigma}{\Delta \rho g H^2} \right)^{1/2}} + \frac{1}{C_{II} \left[ \left( \frac{\varepsilon}{g} \right) \left( \frac{\rho_c}{g \sigma} \right)^{1/4} \right]^n \left[ H \left( \frac{\rho_c g}{\sigma} \right)^{1/2} \right]^{n_2}}}$	(3) Rotating disc column Asymmetric rotating disc column Kühni column Wirtz column Pulsed column Karr column	[10]
$d_{32} = 0.705 \left( \frac{\sigma}{g \Delta \rho} \right)^{0.5} \frac{d_R^{0.8}}{N^{0.185}} \frac{\left( \frac{Q_c}{Q_d} \right)^{0.15}}{\left( Q_c + Q_d \right)^{0.1}}$	(4) Rotating disc column	[11]
$d_{32} = 0.194 \left( \frac{P}{V} \right)^{-0.45} \sigma^{0.766} (\rho_c \mu_c)^{-0.3} \left( \frac{\mu_d}{\mu_c} \right)^{0.07}$	(5) ARDC column	[12]
$d_{32} = 10 \left( \frac{N^4 d_R^4 \rho_c}{\sigma g} \right)^{-0.296} \left( \frac{\mu_c^4 g}{\Delta \rho \sigma^3} \right)^{-0.087} \left( 1 + \frac{V_c}{V_d} \right)^{-0.402}$	(6) Perforated rotating disc column	[13]

## 2. Experimental

### 2.1. Description of equipment

A schematic diagram of the experimental set-up is shown in Fig. 1. The main column section consists of a glass tube of 1430 mm long and 113 mm internal diameter. The column consists of 11 mixing sections and 11 packing sections, and each of them has a height of 140 mm and 200 mm, respectively. The agitators with a diameter of 3.5 mm are

installed in the middle of each mixing section. The packing section with porosity of 97 % is made of stainless steel wire mesh packing. A settler of 168 mm diameter at each end of the column permitted the liquids to coalesce and decant separately. The interface level at the top of the column was controlled automatically by an optical sensor. The dimensions of the column are given in Table 2.

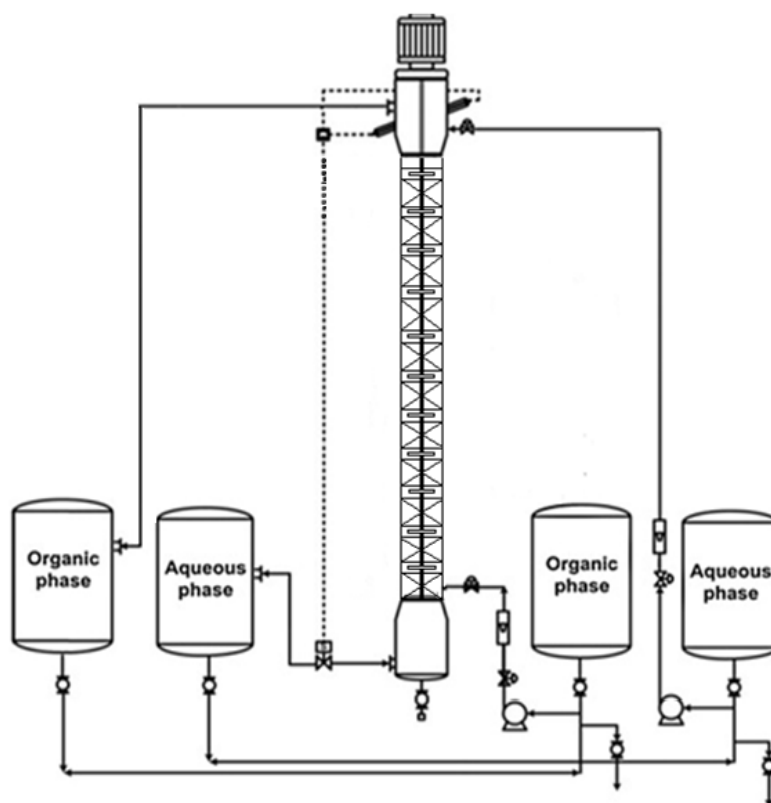


**Figure 1.** A schematic diagram of the Scheibel extraction.

**Table 2**

The main dimensions of the scheibel column.

Item	Symbol	Column dimensions (m)
Column internal diameter	$D_C$	0.113
Compartment height	$h_c$	0.14
Blade length	$D$	0.035
Column active height	$h$	1.43

### 2.2 Liquid systems used

The liquid-liquid systems studied are:

toluene-water (high interfacial tension), n-

butyl acetate-water (medium interfacial

tension), and n-butanol-water (low interfacial tension). These systems are recommended by the European Federation of Chemical Engineering (E.F.C.E.) as official test systems

for liquid extraction. Distilled water was used as a continuous phase in the experiments. The physical properties of the liquid-liquid systems are given in Table 3.

**Table 3**

Physical properties of systems studies [14].

n-Butanol-water	n-Butyl acetate-water	Toluene-water	Physical property
$\rho_c$ (kg/m <sup>3</sup> )	998.2	997.6	985.6
$\rho_d$ (kg/m <sup>3</sup> )	865.2	880.9	846
$\mu_c$ (mPa S)	0.963	1.0274	1.426
$\mu_d$ (mPa S)	0.584	0.734	3.364
$\sigma$ (mN/m)	36	14.1	1.75

### 2.3. Procedure

Before the experiments, both phases were mutually saturated by circulation through the column. After filling the column with the continuous phase, the agitation and continuous phase flow rates were set to the desired values, and the dispersed phase gradually was allowed to enter into the column up to the selected flow rate. The interface location was then maintained at the desired height using the optical sensor, and the system was allowed to reach the steady state, which necessitated 2-3 changes of column volume.

Drop-sized distribution was determined by the photographic technique using a Nikon D3100 digital camera and comparing the dimensions with the known size of the column internal as a reference. A transparent-sided box was attached to the column and filled with water to avoid reflectance and eliminate the distortion effect of the round column during photography. To determine the size of droplets, the recorded photos were analyzed by Digimizer Image Analysis software. A minimum of 200 drops was analyzed for each experiment. In the case of non-spherical droplets, the major and minor axes,  $d_1$  and  $d_2$ , were measured, and

equivalent diameter  $d_e$  was calculated as follows:

$$d_e = (d_1^2 d_2)^{1/3}$$

Sauter-mean drop diameter  $d_{32}$  is then defined by:

$$d_{32} = \frac{\sum n_i d_i^3}{\sum n_i d_i^2}$$

where  $n_i$  denotes the number of drops with diameter  $d_i$ .

## 3. Results and discussion

### 3.1. Drop-sized distributions

In the present study, normal ( $P_n$ ) and log-normal ( $P_{lg}$ ) probability density functions are chosen for representing the experimental drop-sized distributions. These functions are given by the following equations, in which  $d_i$  is the drop diameter and  $\alpha$  and  $\beta$  are parameters to be fitted.

In technical application, it is important to be able to predict the interfacial area of dispersion, because drop velocities within extraction column as well as settling and coalescing all depend on the drop-sized distribution. In real operating conditions, there is often a distribution that results in drop velocities distribution of the continuous phase and mass transfer between the columns. The

most general definition of the spread of the particle size distribution is a monodisperse or polydisperse distribution. A monodisperse distribution is one in which particles are close to a single size, whereas polydisperse suggests a wide range of particle sizes. The collision intensity and turbulence of the system increase with an increase in agitation speed, and consequently, the eddies of the system become smaller. The smaller eddies result in smaller drops. Bouyiotis and Thornton [15] measured drop-sized distribution at the bottom of a mixing vessel, and found that a normal distribution fits the data:

$$f_n(d_{vs}) = \frac{1}{s(\pi)^{1/2}} \exp\left(-\frac{(d - \bar{d})^2}{2s^2}\right) \quad (1)$$

where  $f_n(d_{vs})$  is the probability density,  $s$  is the standard deviation, and  $\bar{d}$  is the arithmetic mean drop-sized distribution.

The log-normal distribution which derives from the normal distribution is defined as follows:

$$P_n(d_i) = \frac{1}{\sqrt{2\pi}\alpha} \exp\left(-\frac{1}{2}\left(\frac{d_i - \beta}{\alpha}\right)^2\right) \quad (2)$$

where  $\alpha$  is the standard deviation and  $\beta$  is the mean. This distribution is well known as "bell-shaped" curve.

The log-normal distribution is obtained from the normal distribution by replacing the independent variable with the logarithm of the particle diameter. The number of particles with diameters between  $d_i+d(d_i)$  is as follows:

$$P_n(d_i) d(d_i) = \frac{1}{\sqrt{2\pi}\alpha} \exp\left[-\frac{1}{2}\left(\frac{(\ln d_i - \beta)}{\alpha}\right)^2\right] \frac{d(d_i)}{d_i} \quad (3)$$

So, the log-normal number of frequency distribution can be conveniently expressed as follows:

$$P(\ln) = \frac{1}{\sqrt{2\pi}\alpha d_i} \exp\left[-\frac{1}{2}\left(\frac{(\ln d_i - \beta)}{\alpha}\right)^2\right] \quad (4)$$

where  $\alpha$  and  $\beta$  are the standard deviation and the mean of the log normal distribution, respectively.

Number density in each test was measured according to the following equation:

$$P_n = \frac{\text{number of drop-sized of class } i}{\text{total number of drops}} \quad (5)$$

The effect of rotor speed on the drop-sized distribution is shown in Fig. 2a.

As seen in this figure, the size distribution clearly shifts toward the left upon an increase in agitation speed, thus indicating that smaller drops and more uniform distributions are obtained in more turbulent conditions. The shear energy imposed by the impeller on the droplets during their ascension accounts for this breakup, and since such energy grows with the agitation speed, the drop breakup frequency increases.

With increasing rotor speed, possibility of drops collision with mixer increases and also produces more eddies energy that cause more drops break; as a result, the area under the curve decreases due to forming smaller drops. In Fig. 2a., it is specified that with decreasing interfacial tension, the area under distribution curve decreases, showing the decreasing size and uniformity of drops.

The effect of velocity of the dispersed and continuous phases on the drop-sized distributions is shown in figures 2b and 2c., respectively. No significant effects are observed for the velocity of the dispersed and continuous phases for the operational conditions investigated.

The effect of dispersed phase velocity on the drop-sized distribution is shown in Fig. 2b. for some systems. A significant change in

the drop-sized distribution will not be observed as there is a decrease in dispersed phase velocity, because the distribution of the dispersed phase in velocity is the same everywhere, although different in every round, the average diameter of the drop-sized distribution of the drops is the same. By changing the interfacial tension, the distribution curve hardly indicates any smaller and more consistent drops. For example, since the tension is lower, Butyl-acetate-water area under the curve Butanol is not great.

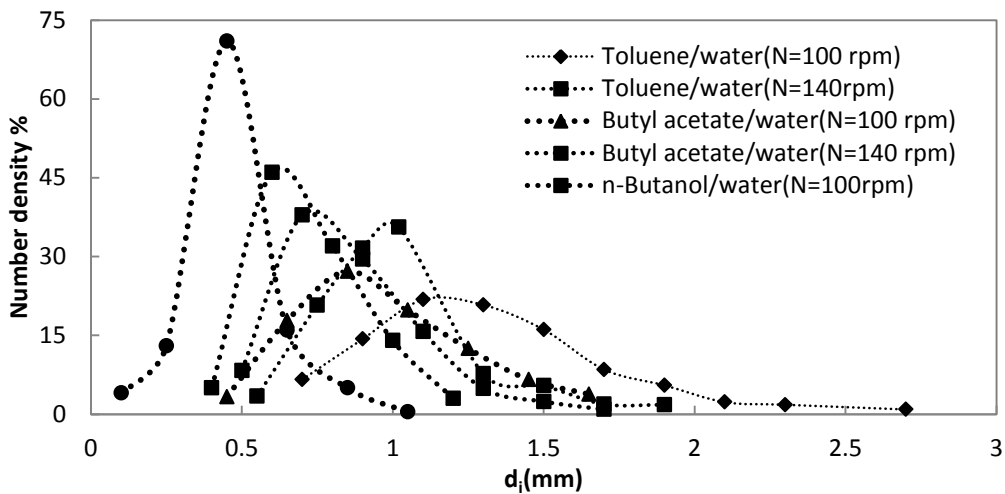
The effect of continuous phase velocity on the drop-sized distribution is shown in Fig. 2c. for some systems. It is known that the

continuous phase velocity does not have any effect on the drop-sized distribution and the distribution is the same everywhere. The drop-sized distribution is appropriately described using the normal and log-normal probability density functions [15-17] and for a Scheibel extraction column, it is as follows:

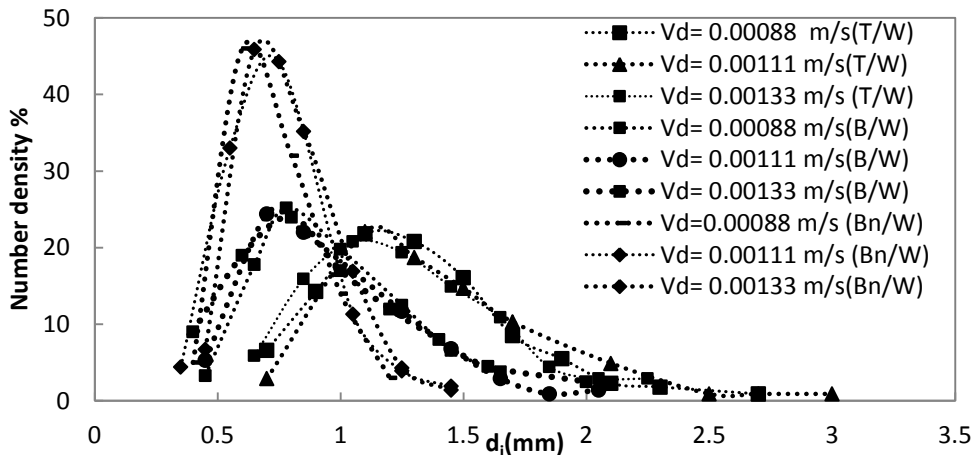
$$P_n(d_i) = \frac{1}{1.62\pi\alpha} \exp\left(-\frac{(d_i - \beta)^2}{2\alpha^2}\right) \quad (6)$$

$$P_{ln}(d_i) = \frac{1}{1.72\pi\alpha d_i} \exp\left(-\frac{(\ln(d_i) - \beta)^2}{2\alpha^2}\right) \quad (7)$$

where  $d_i$  is the diameter of each drop and  $\alpha$  and  $\beta$  are parameters to be fitted.



(a)



(b)

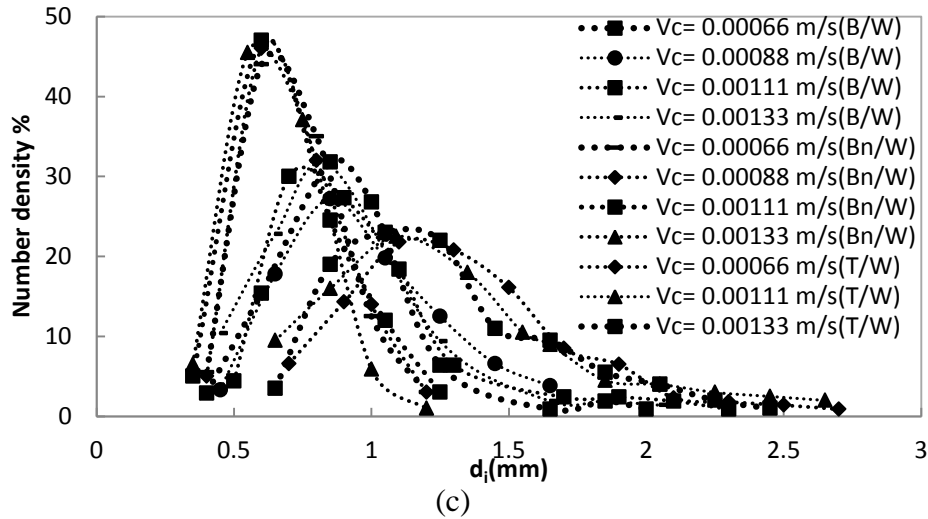


**Figure 2.** Effect of operating parameters on the drop-sized distribution: (a) Rotor speed, (b) Dispersed phase velocity, and (c) Continuous phase velocity.

At first, the value of  $d_i$  as a function of number density was used in the fitting of normal and log-normal distributions for the data set with the aid of the LABFITT software, determining parameters  $\alpha$  and  $\beta$  for each set

$$\alpha = 31.77 \left( \frac{ND^2 \rho_d}{\mu_d} \right)^{0.26} \times \left( \frac{\mu_c^4 g}{\Delta \rho \sigma^3} \right)^{0.33} \times \left( \frac{\sigma}{ND \mu_c} \right)^{1.1} \quad (8)$$

$$\beta = 0.01 \left( \frac{ND^2 \rho_d}{\mu_d} \right)^{-1.64} \times \left( \frac{\mu_c^4 g}{\Delta \rho \sigma^3} \right)^{-1.31} \times \left( \frac{\sigma}{ND \mu_c} \right)^{-3.49} \times \left( 1 + \frac{V_c}{V_d} \right)^{0.09} \quad (9)$$

$$\alpha = 6.14 \left( \frac{ND^2 \rho_d}{\mu_d} \right)^{0.72} \times \left( \frac{\mu_c^4 g}{\Delta \rho \sigma^3} \right)^{0.56} \times \left( \frac{\sigma}{ND \mu_c} \right)^{1.37} \quad (10)$$

$$\beta = 0.01 \left( \frac{ND^2 \rho_d}{\mu_d} \right)^{-1.82} \times \left( \frac{\mu_c^4 g}{\Delta \rho \sigma^3} \right)^{-1.47} \times \left( \frac{\sigma}{ND \mu_c} \right)^{-3.67} \times \left( 1 + \frac{V_c}{V_d} \right)^{0.033} \quad (11)$$

where  $V_d$  and  $V_c$  are velocities of the dispersed and continuous phases,  $N$  is the rotor speed,  $\sigma$  is the interfacial tension,  $\mu_c$  is viscosity of the continuous phase,  $\rho_d$  and  $\mu_d$  are density and viscosity of the dispersed phase,  $\Delta \rho$  is density difference between two phases, and  $g$  is the acceleration due to gravity ( $9.8 \text{ m/s}^2$ ).

In order to evaluate the validity of the obtained absolute value of the average

of the studied operation condition. Correlations made between (8)-(9) and (10)-(11) using the Eviews software and then constant parameters are for normal and log-normal distributions, respectively.

relative error, (AARE %) was calculated using the following equation:

$$\text{AARE \%} = \frac{1}{n} \sum_{k=1}^n \left| \frac{p_i(d) \text{ exp} - p_i(d) \text{ cal}}{p_i(d) \text{ exp}} \right| \times 100 \quad (12)$$

where  $n$  is the number of data point, and  $p_i(d) \text{ (exp)}$  and  $p_i(d) \text{ (cal)}$  represent the experiment and calculation of Eqs. (6)-(7), respectively.

According to the obtained relationships for  $\alpha$  and  $\beta$ , rotor speed and interfacial tension have the key role in the calculation of the drop-sized distribution. As it stands by increasing the rotor speed, the amounts of  $\alpha$  and  $\beta$  will decrease; as a result, the possibility of establishment of drops with a smaller size will increase. The values of  $\alpha$  and  $\beta$  are shown in Table 4.

**Table 4**  
Comparison made between ARRE numbers.

Function	Fitted parameter	AARE %
Normal( $p_n$ )	$\alpha$	8
	$\beta$	11.78
Log-normal( $p_{ln}$ )	$\alpha$	10.5
	$\beta$	13.89

### 3.2. Predictive correlation for mean drop-sized distribution

Further, the drop-sized distribution along with the dispersed-phase interfacial area for mass transfer is determined; as a result, both of the dispersed phase and the mass transfer coefficient phase are always affected. Therefore, if we could predict drops as a function of the geometry column, it is important to operate parameters and predict the physical properties of liquid-liquid systems to analyze the design performance of Scheibel extraction columns. In columns where the number of drops is allot, the drops normally deal with different diameters.

The Sauter-mean drop diameter can be considered as the ratio of the particle volume-to-surface area in a distribution which may have physical significance in some applications. So, it is better to use the Sauter-mean drop diameter to calculate mean drop-sized distribution. The mean drop-sized distribution by Eq. (13) is obtained as follows:

$$d_{32} = \frac{\sum_{i=1}^{i=n} n_i d_i^3}{\sum_{i=1}^{i=n} n_i d_i^2} \quad (13)$$

$d_i$  is the diameter of each drop, which can be measured in each trial by shooting.

Generally, the size of diameter measured in different operating conditions can be found by using a mathematical model to calculate changes in the drop.

Drop-sized distribution depends on various factors, such as the geometry of the blade, blade speed, the blades in the container, the feed phase, and physical properties phases [18].

Fig. 3 shows the effect of rotor speed on the sauter-mean drop diameter. As seen in this figure, rotor speed has a strong effect on the mean drop-sized distribution. An increase in rotor speed leads to higher shear stress and intense drop breaking; consequently, the sauter-mean drop diameter will decrease. However, at high volume of rotor speed, the fall in drop-sized distribution is gradual, and it could be conjectured that further breakup of dispersed phase droplet into smaller one is limited.

In the mixer, drops formed by a 'break-up' of dispersed phase in the shear field in other parts of the flow drops are coalescing, and mixer speed has a strong effect on the drop-sized distribution. The velocity fluctuations over the surface of a drop cause deformations in relation to the scale of the small eddies. Break-up will occur by the dissipative force exceeding the restoring forces. Increasing speed to more mixing shear forces on the drops improves breakup, thus reduces the drop-sized distribution. Reduced tension also leads to smaller drops because the drops' coalescence is low. At lower speeds, the changes of the mean drop-sized distribution are more noticeable, because the drops will be



less broken for low rotor speed, and in return, the drops are very small at higher speeds and

the mean drop-sized distribution of drops is desired in a certain amount.

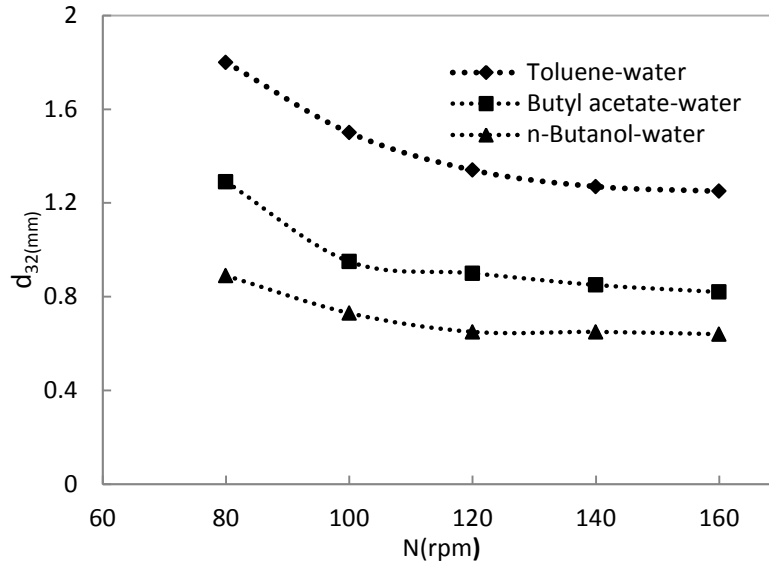


**Figure 3.** Effect of rotor speed on Sauter mean drop diameter ( $V_d=V_c=8.8 \times 10^{-4}$ (m/s)).

The effect of the continuous phase velocity on the sauter-mean drop diameter is illustrated in Fig. 4. As seen in this figure, no significant effect is observed for the continuous phase velocity. Increase of continuous phase speed slows down the movement of dispersed phase drops and increases residence time of drops, and so drops' coalescence increases; however,

an increase in continuous phase speed has no effect on mean drop-sized distribution. It can be said that the existence of mixer in different parts of the column has neutralized the effect of the increase on continuous phase speed. So, the mean drop diameter slightly increases with an increase in continuous phase velocity.

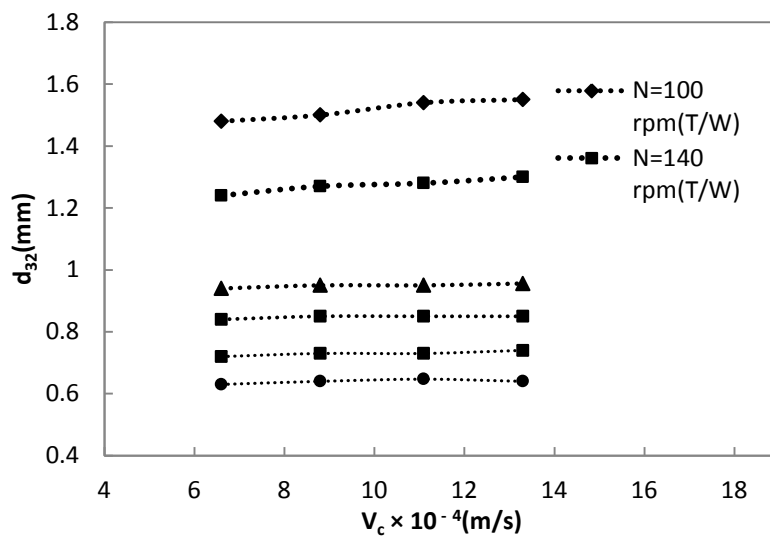


**Figure 4.** Effect of continuous phase velocity on the Sauter-mean drop diameter ( $V_d=8.8 \times 10^{-4}$ (m/s)).



Fig. 5 illustrates the effect of dispersed phase velocity on the mean drop-sized distribution. The mean drop-sized distribution increases with an increase in the dispersed phase velocity.

A higher dispersed-phase velocity leads to not only a larger drop formation diameter, but also to higher coalescence frequencies. Dynamics and mass transfer in a liquid-liquid extraction column are essentially determined by the behaviour of the dispersed phase [19]. By Increasing the speed of dispersed phase, holdup in column increases and possibility of strikes between the drops will increase; thus,

the coalescence of drops will be faster and the mean drop-sized distribution will be bigger [15,20]. Gradients of intensification in the mean drop-sized distribution slow down after  $11.1 \times 10^{-4}$  (m/s) speed desiring a certain amount, because dispersed phases' drops stick inside the packings, slowing down the speed of drops rising. Therefore, there is a possibility of flooding and the phases inversion phenomenon at column. However, it is clear that the effect of the dispersed phase on the drop-sized distribution is much smaller than that of the mixing speed.

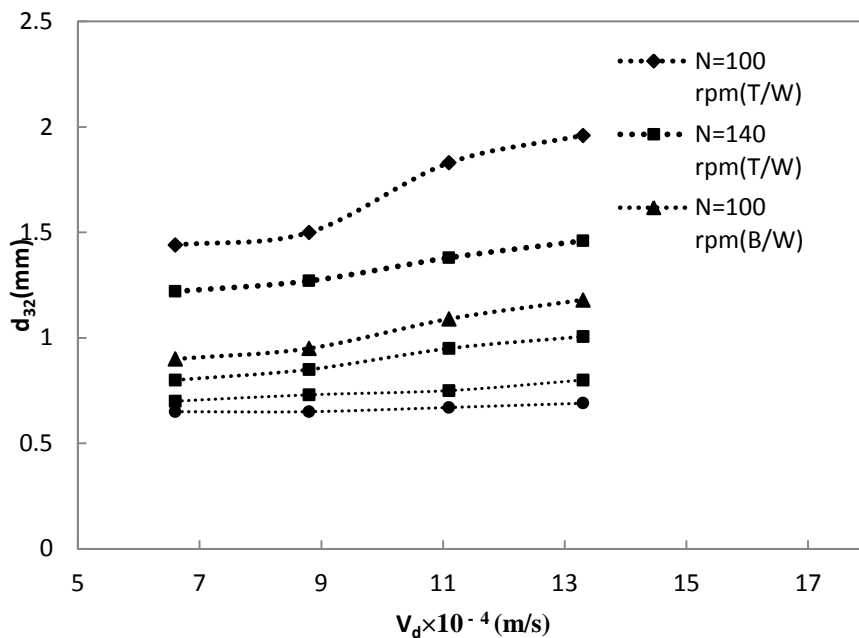


Figure 5. Effect of dispersed phase velocity on the Sauter-mean drop diameter ( $V_c = 8.8 \times 10^{-4}$  (m/s)).

So far, many correlations have predicted the determined Sauter mean drop diameter ( $d_{32}$ ) in other mechanically agitated extraction column, but there is a little correlation in a

Scheibel extraction column. Shefeng Yaun and Jin [21] predicted a correlation for Sauter-mean diameter in a modified Scheibel extraction column:

$$\frac{d_{32}}{D} = 781.6 \left( \frac{Q_d}{ND^3} \right)^{0.065} \left( \frac{\mu_c}{\mu_d} \right)^{0.35} \left( \frac{\Delta p}{\rho_d} \right)^{-1.971} Re^{-1.651}, \quad 0 \leq Re \leq 2500 \quad (14)$$

In the absence of mass transfer, Bonnet and Jeffreys proposed a correlation for Sauter-mean drop diameter in a Scheibel Extractor

[22]:

$$d_{32} = 5.719 \times 10^{-5} \times 10^{(1+1.397\phi_d)} \epsilon^{-0.708} \quad (15)$$

Comparison between the suggested and experimental values using these correlations is shown in Fig. 6a. With the help of correlations (14) and (15), most of experimental data are anticipated with an AARE of about 75 %.

If a characteristic size or size distribution is to be computed for the given conditions, these are only relevant if a dynamics equilibrium between break-up and coalescence is achieved in the contactor. A mathematical model and the empirical relation to predict the true physics accurately is a need to understand the parameters, variables, and factors affecting the parameters, and the impact of these factors on the parameters is desired. In this paper, the effects of operating conditions, such as continuous-phase velocity and dispersed-phase velocity and physical

properties, e.g., interfacial tension of the mixing room, were examined. Analyses of variables affecting the Sauter-mean drop diameter of the functional relationship between these variables and mean drop-sized distribution are conducted as follows:

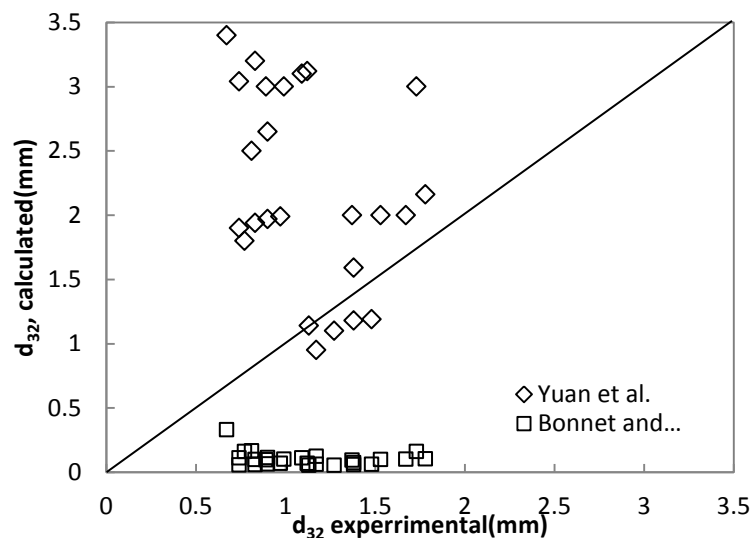
$$d_{32} = f(d_{32}, N, V_d, \sigma, \rho_c, \rho_d, \Delta\rho, \mu_c, \mu_d, D) \quad (16)$$

Using Buckingham Pi theorem for obtaining the equation of the mean drop-sized distribution has formed the dimensionless groups based on operation parameters and physics properties; moreover, by using Eviews software, the constant amounts of empirical correlation will be calculated. Eq. (17) shows the anticipated correlation of the Sauter-mean drop diameter in a Scheibel extraction column:

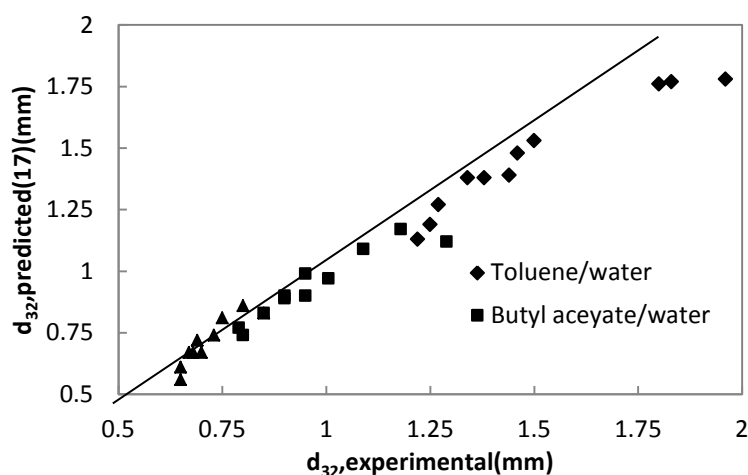
$$\frac{d_{32}}{D} = 0.0043 \left( \frac{V_d}{ND} \right)^{0.25} \left( \frac{\mu_c}{\mu_d} \right)^{-1.77} \left( \frac{\Delta\rho}{\rho_d} \right)^{0.15} \left( \frac{N^4 D^4 \rho_d}{\sigma g} \right)^{0.085} \left( \frac{\sigma}{ND\mu_d} \right)^{0.7}$$

Also, in this correlation, experimental data obtained by Yuan et al. and Bonnet and Jeffreys are used to reduce errors. The comparison of calculation by Eq. (17) and experimental data for mean drop-sized distribution is shown in Fig. 6b. This figure

indicates that the predicted correlation can estimate the mean drop-sized distribution with high precision, and the AARE percent in the predicted values of  $d_{32}$  from experimental data is 9.8 %.



(a)



(b)

**Figure 6.** (a) Comparison between experimental data and correlation [14],[15], (b) Comparison between experimental data and correlation (17).

#### 4. Conclusions

Drop-sized and mean drop-sized distributions were presented for the three liquid-liquid systems in a Scheibel column for a range of rotor speeds and dispersed and continuous phases' velocities. The droplet-sized distribution in the column is usually represented as the average volume-to-surface area, known as the Sauter-mean drop diameter. It is a key variable in the extraction column design. It influences both throughput and specific interfacial areas available for mass transfer, dispersed phase holdup, and flooding conditions. The drop-sized distribution predicted by the statistical approach was compared with experimental data, and the computational fluid dynamics and droplet population balance modeling were used to evaluate the normal and log-normal developed in this study. The results showed that the drop size is dependent on rotor speed and only weakly dependent on the flow rate of the phases. The drop-sized distributions were suitably fitted to the normal and log-normal distribution curves, and empirical correlations were derived to predict the drop-sized distribution as a function of operating variables and physical properties of

the systems. The prediction of the Sauter-mean drop size was shown to be not possible using previous correlations. An empirical expression of the Sauter-mean drop diameter was also proposed.

#### Nomenclature

D	blade length [m].
$d_{32}$	mean drop size [m].
$d_i$	drop diameter [mm].
$d_v$	Sauter mean drop size [m].
d	arithmetic mean drop size.
$f_n$	probability density.
g	gravitational constant ( $=9.81 \text{ m/s}^2$ ).
N	rotor speed [1/s].
$n_i$	number of droplets of mean diameter $d_i$ .
P	probability of number density.
Q	flow rate [ $\text{m}^3/\text{s}$ ].
Re	Reynolds number.
V	superficial velocity [m/s].

#### Greek symbols

$\alpha$	constant parameter of probability of density function.
$\beta$	constant parameter of probability of density function.
$\rho$	density [ $\text{kg m}^{-3}$ ].
$\Delta\rho$	density difference between two phases [ $\text{kg/m}^3$ ].
$\mu$	viscosity [Pa s].
s	standard deviation.

$\sigma$  interfacial tension between two phases [N/m].  
 $\varphi$  holdup.  
 $\bar{\epsilon}$  average energy dispersion per unit mass.

### Subscripts

c continuous phase.  
d dispersed phase.  
n normal probability density function.  
ln log-normal probability density function.

### References

[1] Torab-Mostaedi, M. and Safdari, J., "Mass transfer coefficients in a pulsed packed extraction column", *Chem. Eng. Process: Process Intensification*, **48** (8), 1321 (2009).  
[2] Blass, E., Goldman, G., Hirschmann, K., Mihailowitsch, P. and Pietzsch, W., "Progress in liquid-liquid extraction", *Ger. Chem. Eng.*, **9** (4), 222 (1986).  
[3] Davies, G. A., *Mixing and coalescence phenomena in liquid-liquid systems*, Edited by J. D. Thornton, p. 248 (1992).  
[4] Mohanty, S., "Modeling of liquid- liquid extraction column : A review", *Reviews in Chem. Eng.*, **16** (3), 199 (2000).  
[5] Ma, S. and Li, P., "Reaction extraction of furfural from pentose solutions in a modified Scheibel column", *Chem. Eng. Process: Process Intensification*, **83** (1), 71 (2014).  
[6] Yin, H., Chen, Z. S., Yuan, S. F. and Chen, Z. R., "Study on an ideal start-up model for a modified Scheibel column", *Applied Mathematical Modelling*, **35** (12), 5835 (2011).  
[7] Maa, S., Wollny, S., Voigt, A. and Kraume, M., "Experimental comparison of measurement techniques for drop-sized distributions in liquid-liquid

dispersions", *Exp. Fluids*, **50** (2), 259 (2011).  
[8] Torab-Mostaedi, M., Ghaemi, A. and Asadollahzadeh, M., "Flooding and drop-sized in a pulsed disc and doughnut extraction column", *Chem. Eng. Res. Des.*, **89** (12), 2742 (2011).  
[9] Kumar, A., Steiner, L. and Hartland, S., "Capacity and hydrodynamics of an agitated extraction column", *Ind. Eng. Chem. Process Des. Dev.*, **25** (3), 728 (1986).  
[10] Kumar, A. and Hartland, S., "Unified correlations for the prediction of drop-sized in liquid-liquid extraction columns", *Ind. Eng. Chem. Res.*, **35** (8), 2682 (1996).  
[11] Al-Rahawi, A. M. I., "New predictive correlations for the drop-sized in a rotating disc contactor liquid-liquid extraction column", *Chem. Eng. Technol.*, **30** (2), 184 (2007).  
[12] Kadam, B. D., Joshi, J. B. and Patil, R. N., "Hydrodynamic and mass transfer characteristics of asymmetric rotating disc extractors", *Chem. Eng. Res. Des.*, **87** (5), 756 (2009).  
[13] Hemmati, A., Torab-Mostaedi, M., Shirvani, M. and Ghaemi, A., "A study of drop-sized distribution and mean drop-sized in a perforated rotating disc contactor (PRDC)", *Chem. Eng. Res. Des.*, **96**, 54 (2015).  
[14] Misek, T., Berger, R. and Schroter, J., *Standard Test Systems for liquid extraction*, EFCE Publ. Ser., London, England, p. 46 (1985).  
[15] Moreira, E., Pimenta, L. M., Carneiro, L. L., Faria, R. C. L., Mansur, M. B. and Ribeiro Jr., C. P., "Hydrodynamic behavior of a rotating disc contactor under low agitation conditions", *Chem.*

- Eng. Commun.*, **192** (8), 1017 (2005).
- [16] Chen, W., Ming zhong, L., Chen, L. and Weiyang, L. W., "Measurement and analysis of bimodal drop-sized distribution in a rotor-stator homogenizer", *Chem. Eng. Sci.*, **102** (1), 622 (2013).
- [17] Oliveira, N. S., Silva, D. M., Gondim, M. P. C. and Mansur, M. B., "A study of the drop-sized distributions and hold-up in short Kuhni columns", *Braz. J. Chem. Eng.*, **25** (4), 729 (2008).
- [18] Pacek, A. W., Chamsart, S., Nienow, A. W. and Bakker, A., "The influence of impeller type on mean drop-sized and drop-sized distribution in an agitated vessel", *Chem. Eng. Sci.*, **54** (19), 4211 (1999).
- [19] Dimitrova Al Khani, S., Gourdon, C. and Casamatta, G., "Dynamic and steady state simulation of hydrodynamics and mass transfer in liquid-liquid extraction column", *Chem. Eng. Sci.*, **44** (6), 1295 (1989).
- [20] Samani, M. G., Safdari, J., Haghghi Asl, A. and Torab-Mostaedi, M., "Effect of structural parameters on drop-sized distribution in pulsed packed column", *Chem. Eng. Technol.*, **37** (7), 1155 (2014).
- [21] Yuan, S. , Shi, Y., Yin, H., Chen, Z. and Zhou, J., "An improved correlation of the drop-sized in a modified Scheibel extraction column", *Chem. Eng. Technol.*, **37** (12), 2165 (2014).
- [22] Bonnet, J. C. and Jeffreys, G. V., "Hydrodynamics and mass transfer characteristics of a Scheibel extractor, Part II: Backmixing and stage efficiency", *AIChE J.*, **31** (5), 795 (1985).